Measurements of photon production at ATLAS

Ana Cueto
On behalf of the ATLAS Collaboration

DIS2019, April 8th–12th, 2019, Torino

Outline:

- ★ **Introduction**
- ★ **Inclusive photon cross-section ratios**
- ★ **$\gamma + jet$ @ 13 TeV**
- ★ **Summary**

PROMPT PHOTONS: **Photons not coming from hadron decays**

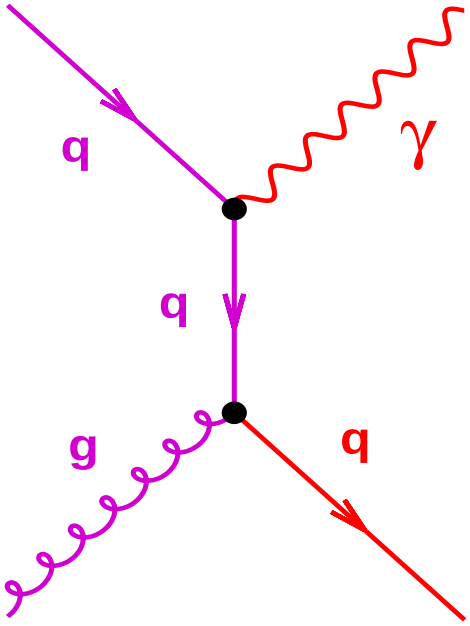

DIRECT

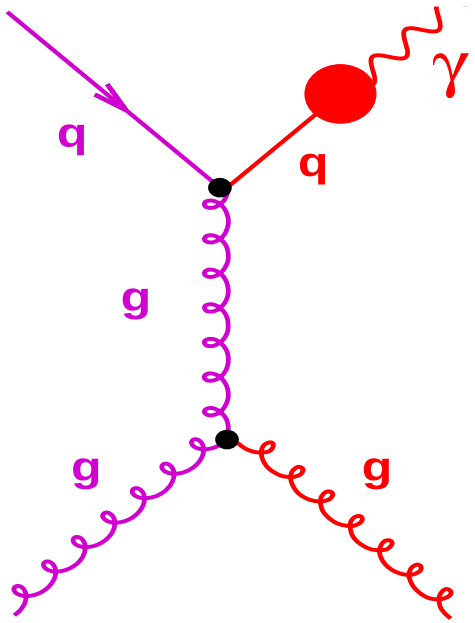

FRAGMENTATION

- Test of pQCD with a hard colorless probe.
  ↪ Sensitivity to gluon PDF at LO through Compton scattering.
- Background of BSM searches and SM measurements (H→ $\gamma\gamma$).
  ↪ BSM: Monophoton/jet, extra dimensions, q^*, exotic neutral particles,...
- Possibilities of studies of inclusive production or in association with jets.
  ↪ Study of the dynamics of the hard process.
  ↪ Useful for improving MC modelling.

Other sources of photons

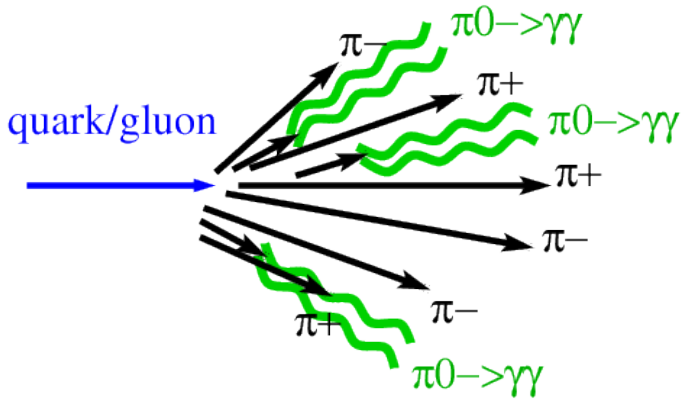

- Photons are copiously produced inside jets due to neutral meson decays.
- In most configurations, these photons are **not isolated**.

PHOTON ISOLATION

★ The isolation requirement suppresses the contribution of photons inside jets: meson decays to pair of photons and fragmentation contribution.

- In general, a fixed-cone isolation requirement is imposed.

$$E_T^{\rm iso} \equiv \sum_i E_T^i < E_T^{\rm max}$$

- Theoretical predictions are greatly simplified if a smooth-cone isolation (Frixione's) criteria is applied.

$$\chi(R) = \epsilon_s \left(\frac{1-\cos R}{1-\cos R_0}\right)^n; \quad E_T^{\rm iso}(R) \leq E_T^\gamma \chi(R)$$

→ Avoid any fragmentation contribution.
→ Impossible experimental implementation.

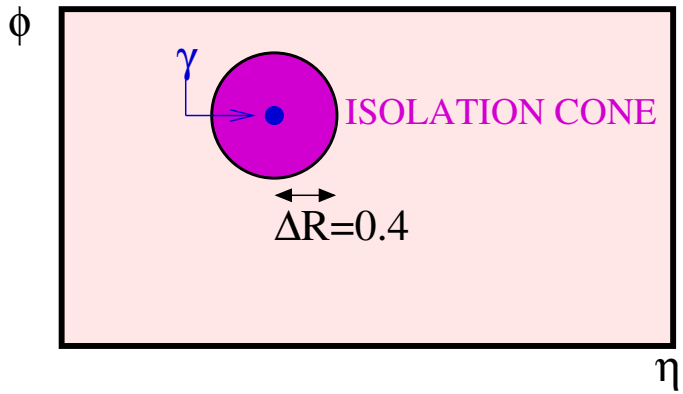

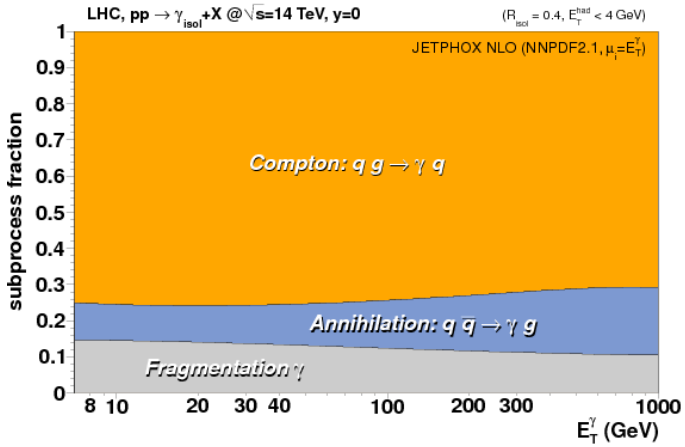

Nucl.Phys. B860(2012) 311-338

Photon isolation in ATLAS and background subtraction

- The isolation transverse energy, E_T^{iso}, is computed from topological clusters (EM and HAD) in a cone of $R = 0.4$ excluding the area centered on the photon cluster ($\Delta\eta \times \Delta\phi = 0.125 \times 0.175$).
- E_T^{iso} is corrected for the photon leakage out of the photon cluster cells and for pile-up and underlying event effects (jet-area method)

→ The isolation requirement is optimized for each analysis.

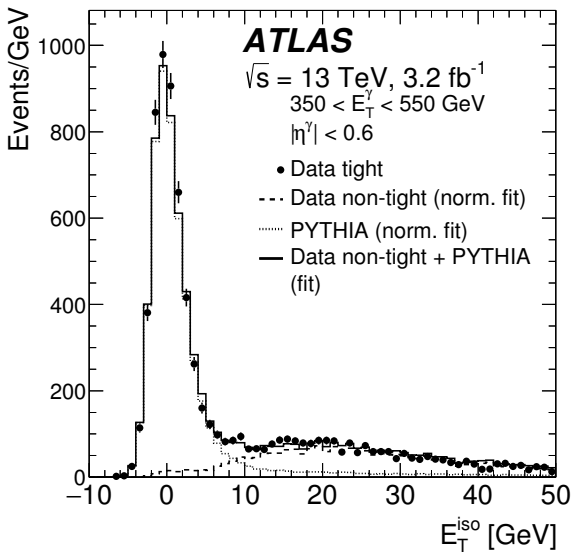

Phys. Lett. B 780 (2018) 578

→ Residual background contribution even after the application of the isolation and tight-ID requirements coming from jets misidentified as photons or Drell-Yan processes.

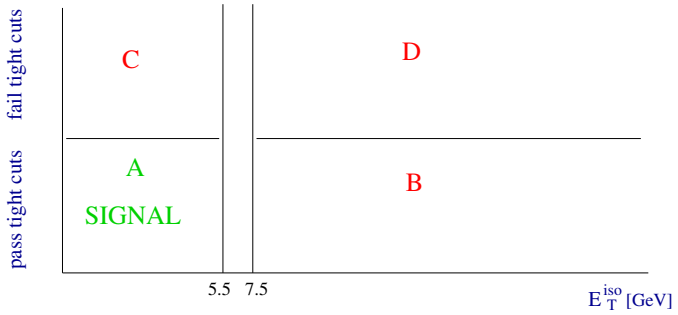

- Data-driven 2D-sideband method:
$$N_A^{\mathrm{sig}} = N_A - R_{\mathrm{bg}} \frac{(N_B - \epsilon_B N_A^{\mathrm{sig}})(N_C - \epsilon_C N_A^{\mathrm{sig}})}{(N_D - \epsilon_D N_A^{\mathrm{sig}})}$$
- Signal leakage fractions (ϵ_K) and correlations for the background between regions (R_{bg}) taken into account.

Inclusive cross-section ratios between $\sqrt{s} = 13$ and 8 TeV

JHEP 06 (2016) 005

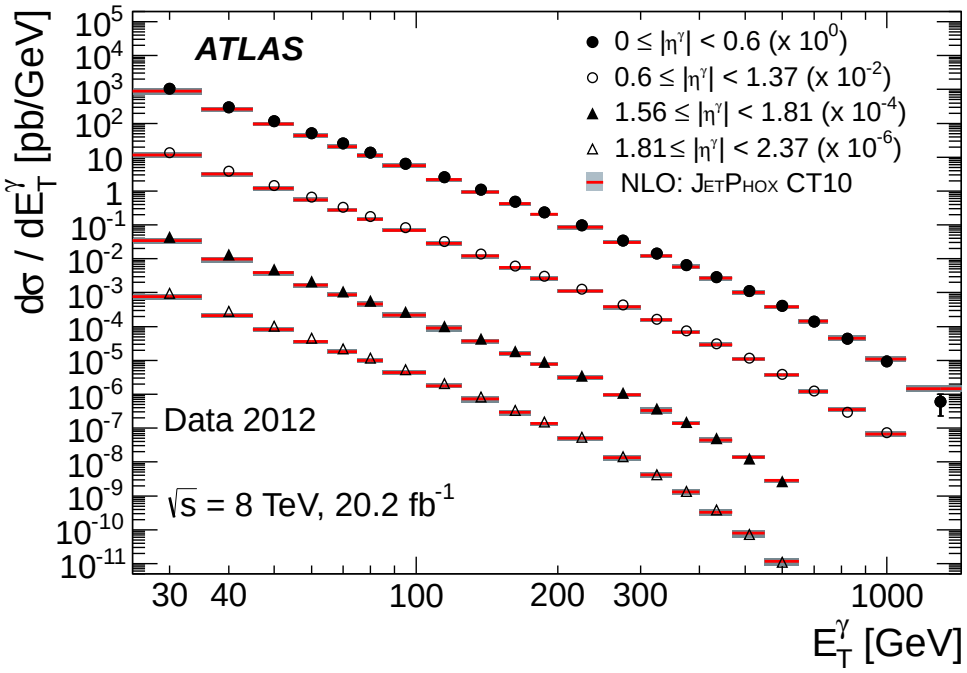

Phys. Lett. B 770 (2017) 473

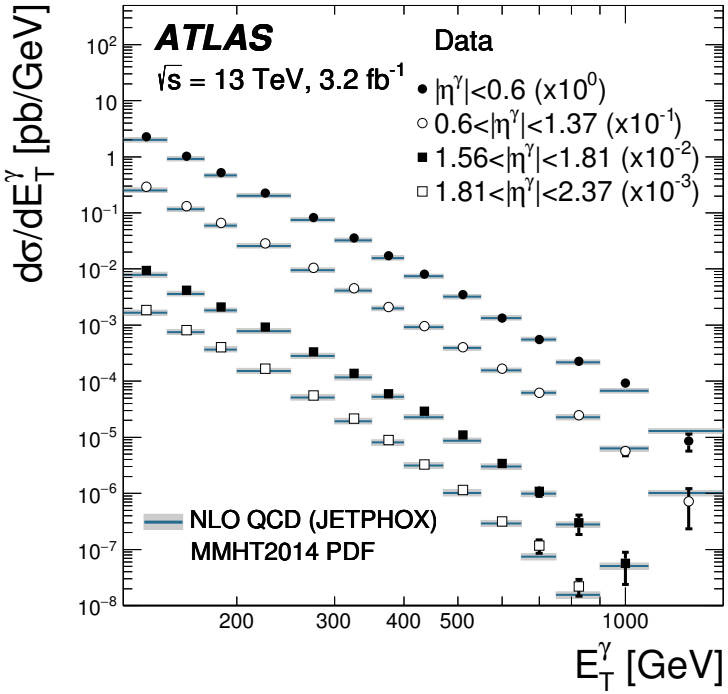

- Measurements of inclusive isolated-photon production performed at 8 and 13 TeV in an overlapping phase-space region.
- Comparisons to NLO QCD limited by the size of the theoretical uncertainties (typically larger than the experimental uncertainties).
- More stringent test of theory through cross-section ratios at different $\sqrt{s}$.
  $\hookrightarrow$ It also tests directly the evolution between both $\sqrt{s}$
- Important to properly take into account the correlation between uncertainties

Inclusive cross-section ratios between $\sqrt{s} = 13$ and 8 TeV

$E_{\mathrm{T}}^{\gamma} > 125$ GeV, $|\eta^{\gamma}| < 2.37 \notin 1.37 < |\eta^{\gamma}| < 1.56$
$E_{\mathrm{T}}^{\mathrm{iso}} < 4.2 \cdot 10^{-3} E_{\mathrm{T}}^{\gamma} + 4.8$ GeV in $\Delta R = 0.4$

- Full correlation of uncertaintes is only used when justified.
  ↪ Mainly in the estimation of the photon energy scale (extra uncertaintes at 13 TeV for changes in configuration of the ATLAS detector)
  ↪ Other uncertainties taken conservatively as uncorrelated: changes in running conditions, optimization of the photon identification or differences in the estimation of the systematic uncertainties.

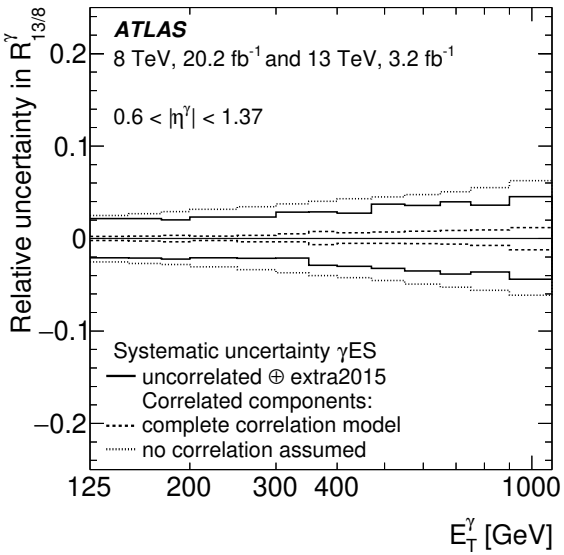

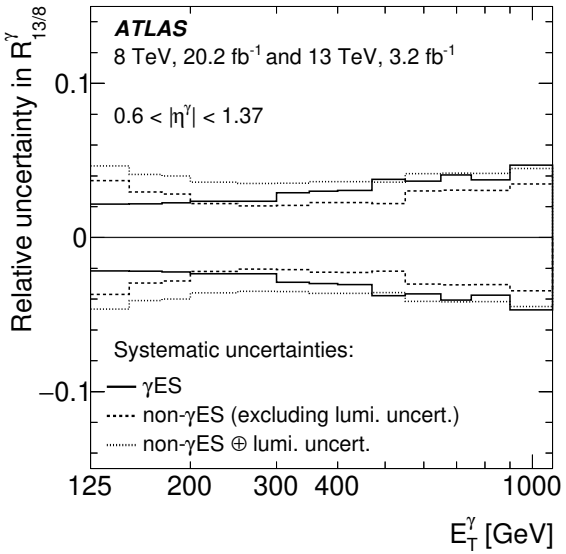

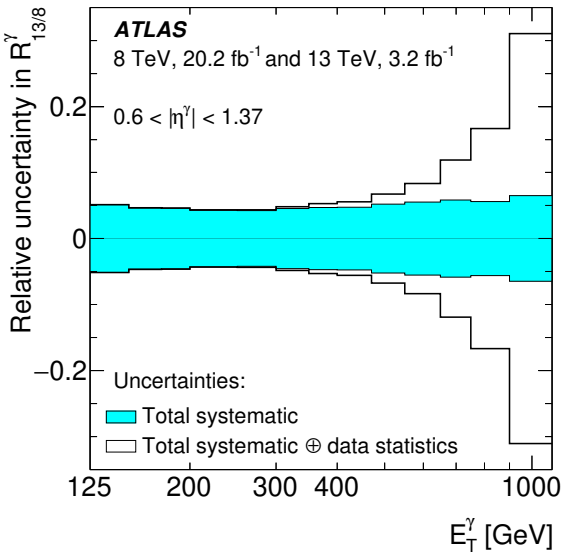

Correlated unc. for γES Systematic uncertainties Syst. and Stat. unc.

- Luminosity uncertainty (2.8%, uncorrelated between $\sqrt{s}$) plays an important role.

arXiv:1901.10075

Inclusive cross-section ratios between $\sqrt{s} = 13$ and 8 TeV

- Double ratio free of luminosity uncertainty.

arXiv:1901.10075

$$D^{\gamma/Z}_{13/8} = \frac{R^{\gamma}_{13/8}(E^{\gamma}_{T})}{\sigma^{\mathrm{fid}}_{Z}(13\,TeV)/\sigma^{\mathrm{fid}}_{Z}(8\,TeV)}$$

- Measures the increase of cross section for isolated photon production with $\sqrt{s}$ normalised to the increase of Z boson with $\sqrt{s}$.
- $\sigma^{\mathrm{fid}}_{Z}(13\,TeV)/\sigma^{\mathrm{fid}}_{Z}(8\,TeV)$ measured by ATLAS in JHEP 02 (2017) 117

$$1.537 \pm 0.001 \quad (\mathrm{stat}) \pm 0.010 \quad (\mathrm{syst}) \pm 0.044 \quad (\mathrm{lumi})$$

- Systematic uncertainty of 0.7% dominated by lepton efficiency; three times smaller than systematic uncertainties in $R^{\gamma}_{13/8}$. Small correlations between electron and photon energy scale can be safely neglected.

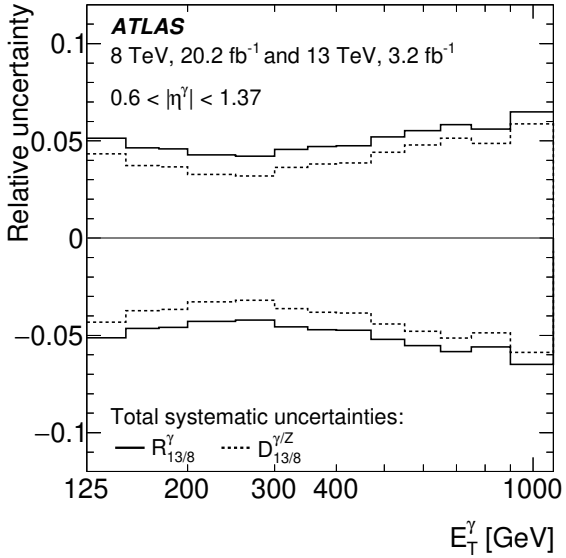

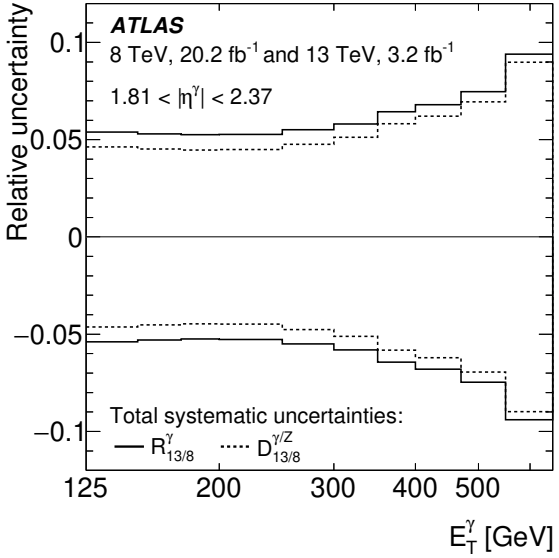

Inclusive cross-section ratios between $\sqrt{s} = 13$ and 8 TeV

- Theoretical predictions for $R^{\gamma}_{13/8}$ at NLO QCD obtained using JetPhox.

↪ All relevant scales set to E^{γ}_{T}; 5FS; BFG II quark/gluon-to-photon fragmentation functions; several PDFs investigated

↪ Uncertainties due to scale variations, PDF, α_s, beam energy and non-perturbative corrections are considered as correlated between both $\sqrt{s}$

→ Large reduction of the theoretical uncertainties compared to the individual inclusive photon measurements.

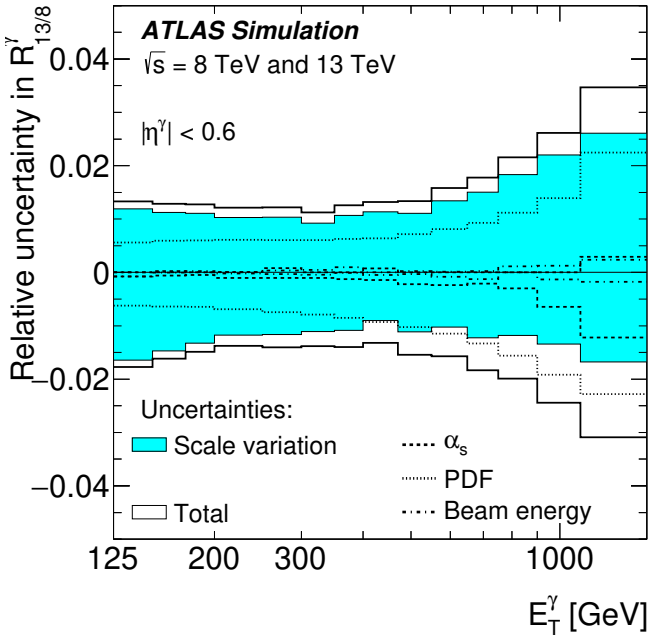

- $\sigma_Z^{\mathrm{fid}}(13\,TeV)/\sigma_Z^{\mathrm{fid}}(8\,TeV)$ predictions computed with DYTURBO at NNLO QCD

↪ Scale uncertainties considered as uncorrelated between $\sigma_Z^{\mathrm{fid}}(13\,TeV)/\sigma_Z^{\mathrm{fid}}(8\,TeV)$ and $R^{\gamma}_{13/8}$

↪ PDF and α_s-induced uncertainties considered as fully correlated

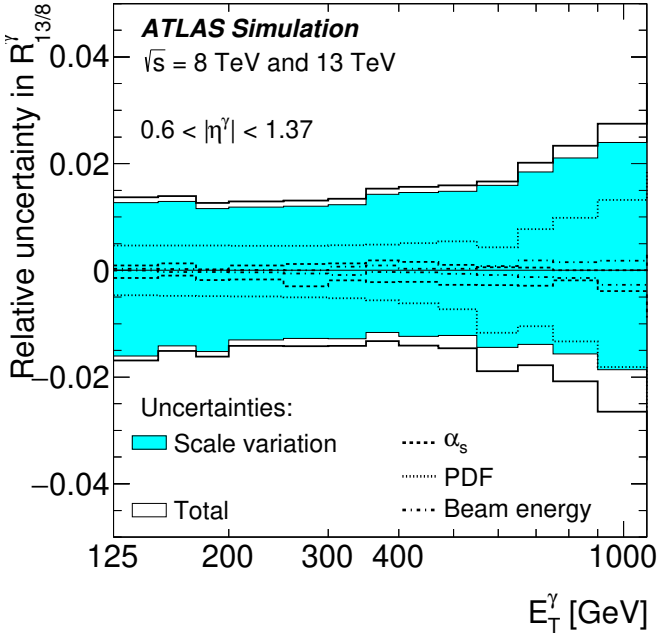

arXiv:1901.10075

Inclusive cross-section ratios between $\sqrt{s} = 13$ and 8 TeV

- Measured $R^{\gamma}_{13/8}$ compared to NLO predictions

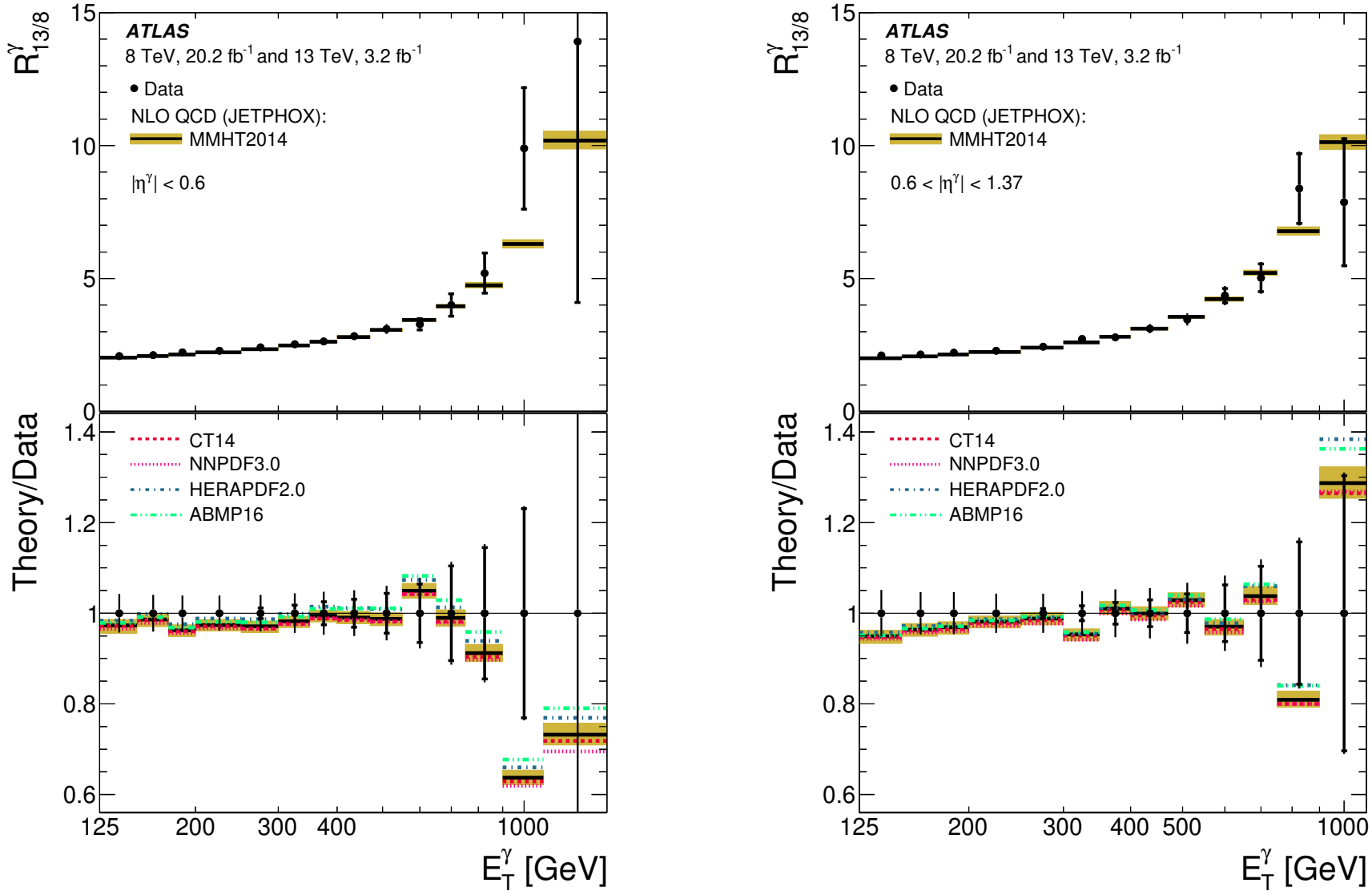

↪ NLO predictions agree with the measured $R^{\gamma}_{13/8}$ within the reduced theoretical uncertainties (2-4%).

arXiv:1901.10075

Inclusive cross-section ratios between $\sqrt{s} = 13$ and 8 TeV

- Measured $D^{\gamma/Z}_{13/8}$ compared to predictions

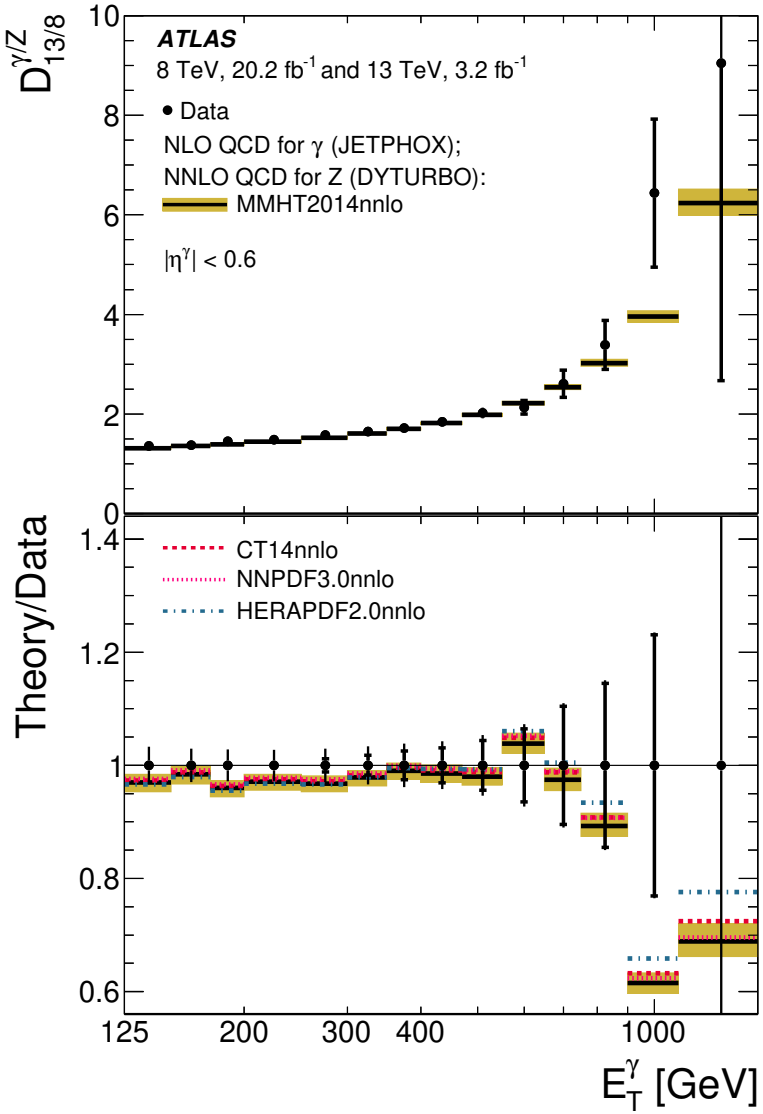

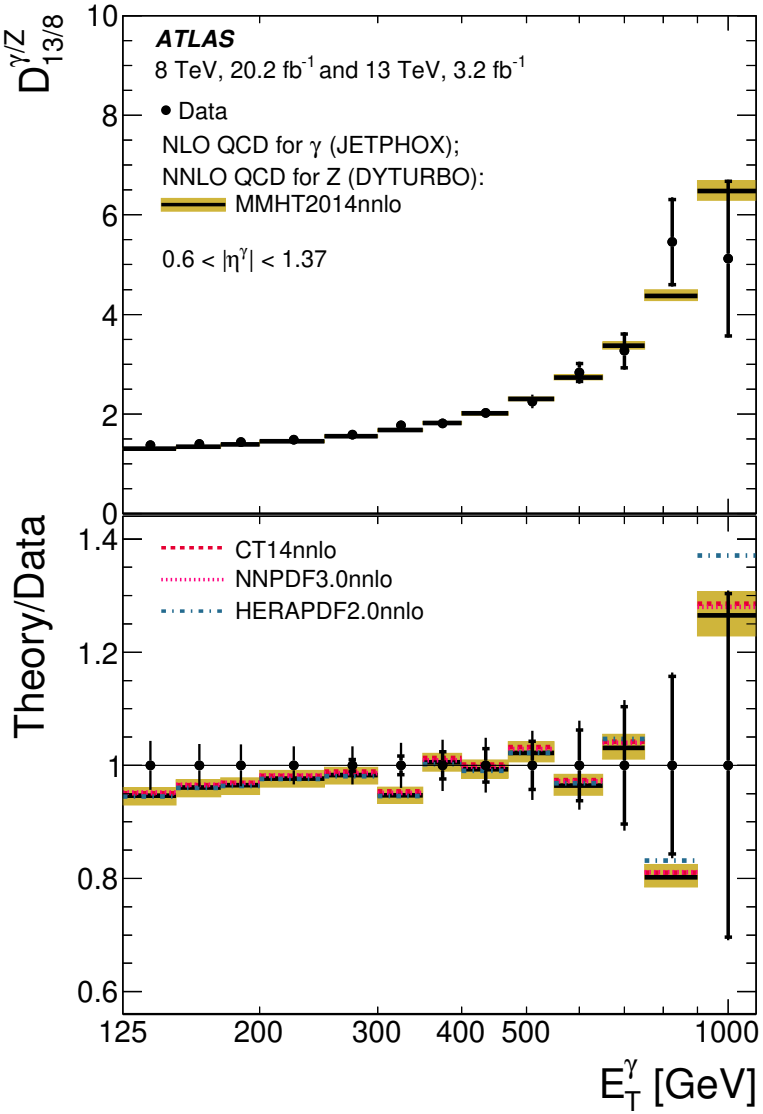

↪ NLO predictions agree with the measured $R^{\gamma}_{13/8}$ within the reduced experimental uncertainties.

arXiv:1901.10075

$pp \to \gamma + jet$ at $\sqrt{s} = 13$ TeV

- Measurement of the differential cross sections as functions of E_T^γ, p_T^{jet}, $\Delta\phi^{\gamma-\text{jet lead}}$, $m^{\gamma-\text{jet}}$ and $|\cos\theta^\star|$ with $\mathcal{L} = 3.2$ fb^{-1}.

E_T^γ >125 GeV, $|\eta^\gamma| < 2.37 \notin 1.37 < |\eta^\gamma| < 1.56$

E_T^{iso} <$4.2 \cdot 10^{-3} E_T^\gamma + 10$ GeV, $\Delta R^{\gamma-j} > 0.8$

$p_T^{jet} > 100$ GeV, $|y^{jet}| < 2.37$

Unbiased selection for $\cos\theta^\star$ and $m^{\gamma-\text{jet}}$:

$|\eta^\gamma| + |y^{jet}| < 2.37$, $m^{\gamma-\text{jet}} > 450$ GeV

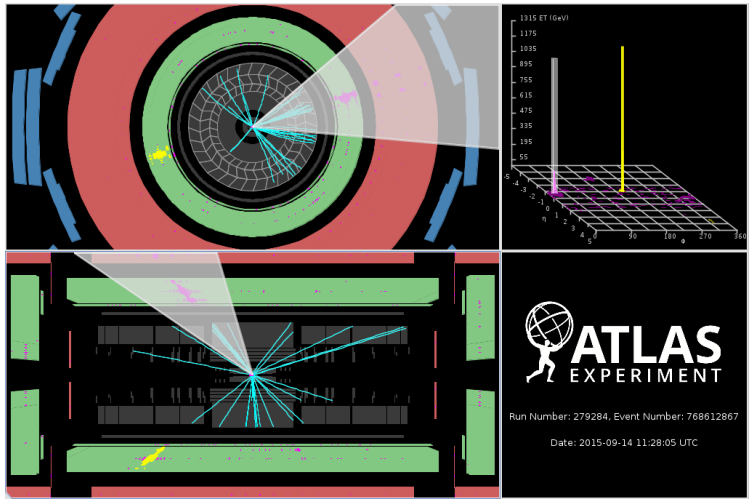

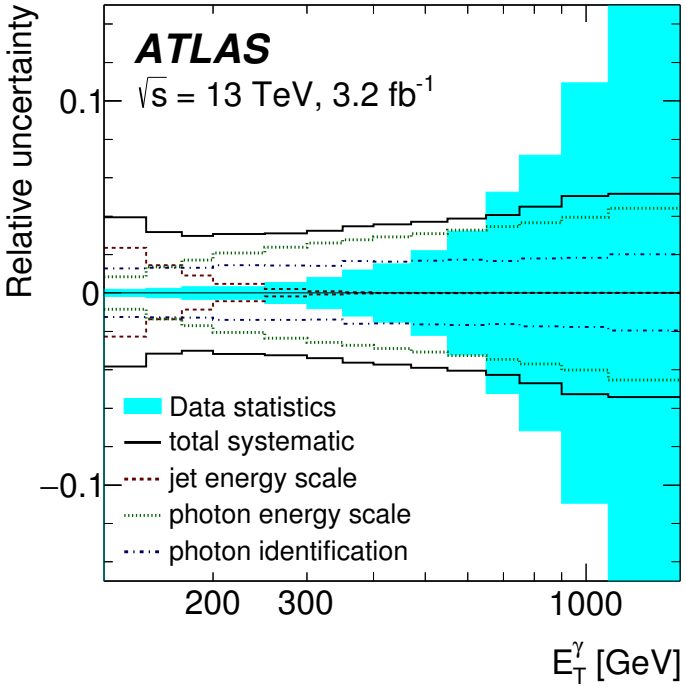

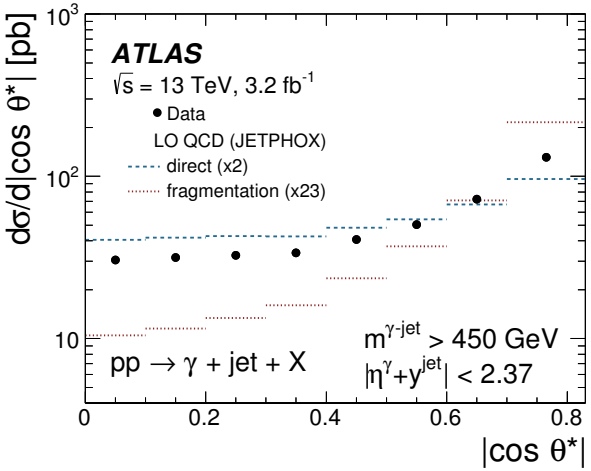

- Total systematic uncertainty (4–5%) dominated by jet energy scale, photon energy scale and photon identification.
- Dominance of the t-channel quark exchange (direct contribution)

Phys. Lett. B 780 (2018) 578

$pp \to \gamma + jet$ at $\sqrt{s} = 13$ TeV

- Comparison of the measured cross sections to the normalized LO SHERPA (multileg) and PYTHIA predictions, and NLO predictions from SHERPA (+ PS) and JETPHOX (corrected for non-perturbative effects) Phys. Lett. B 780 (2018) 578

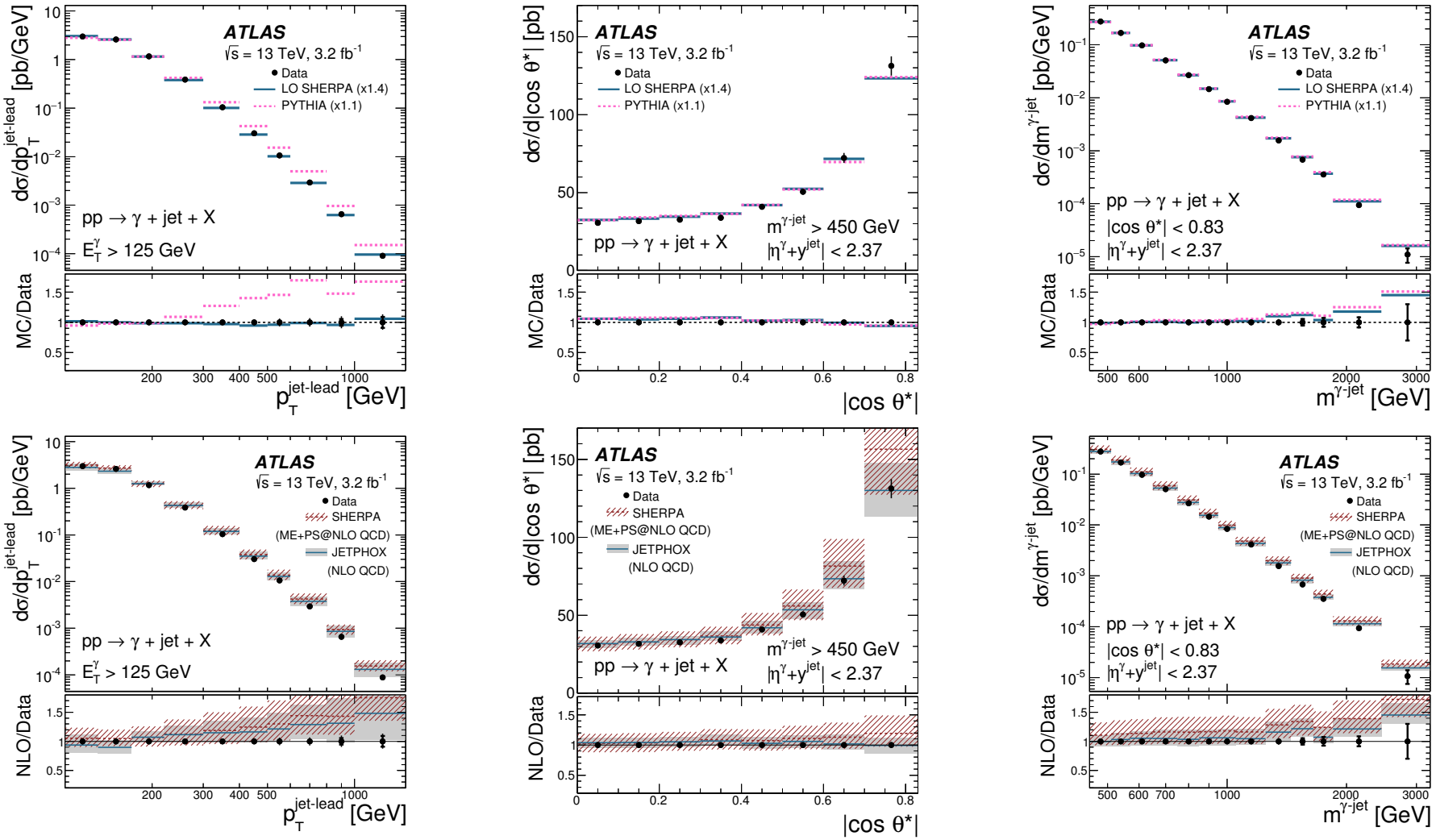

▶ First measurement of photon + jet production in pp collisions at $\sqrt{s} = 13$ TeV.

$pp \to \gamma + jet$ at $\sqrt{s} = 13$ TeV

Impressive improvement on the $p_{\mathrm{T}}^{\mathrm{jet}}$ description by higher-order predictions
↪ arXiv:1904.01044 (X. Chen, T. Gehrmann, N. Glover, M. Hoefer, A. Huss)

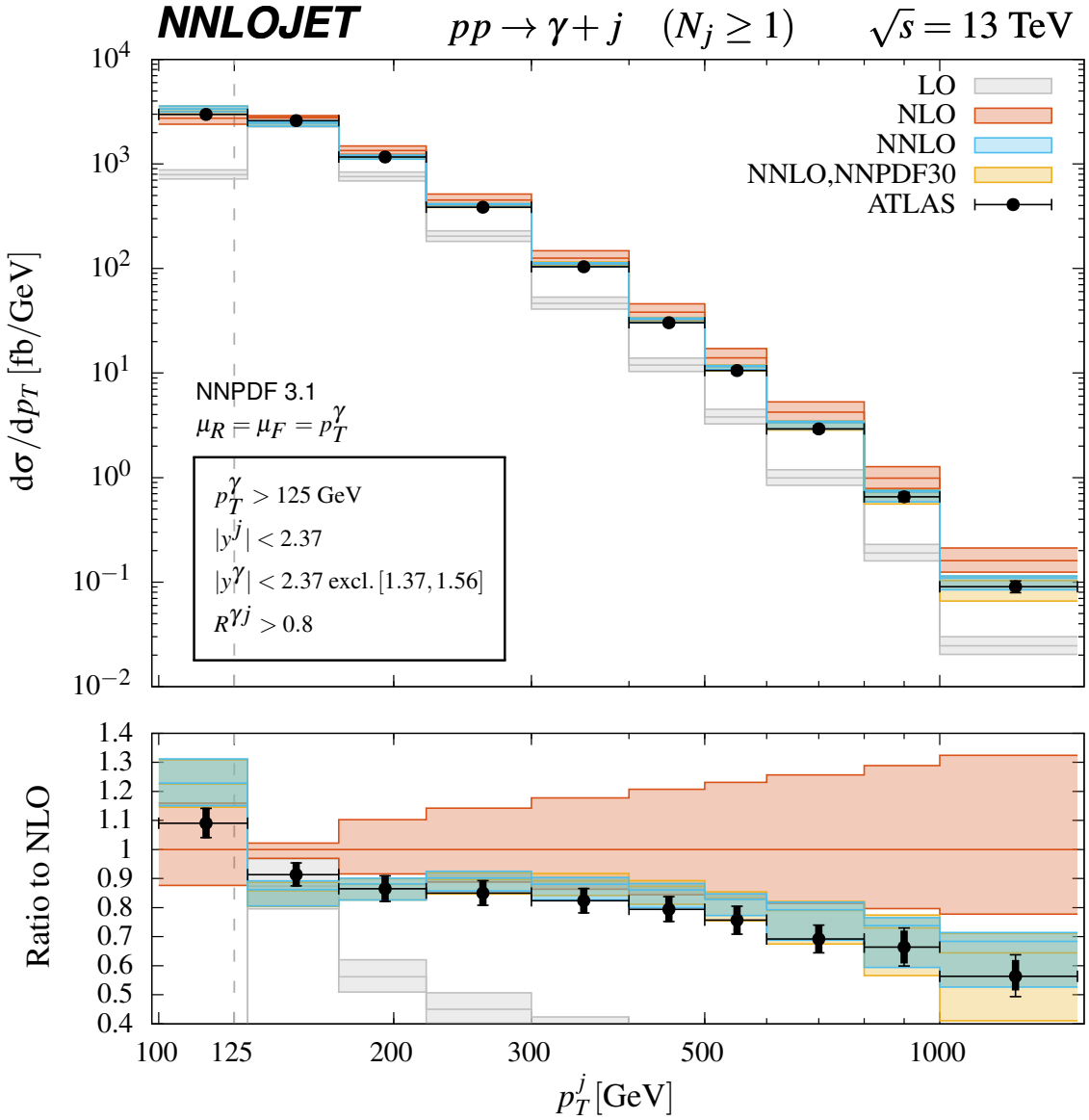

Impressive improvement on the $p_{\mathrm{T}}^{\mathrm{jet}}$ description by higher-order predictions
↪ arXiv:1904.01044 (X. Chen, T. Gehrmann, N. Glover, M. Hoefer, A. Huss)

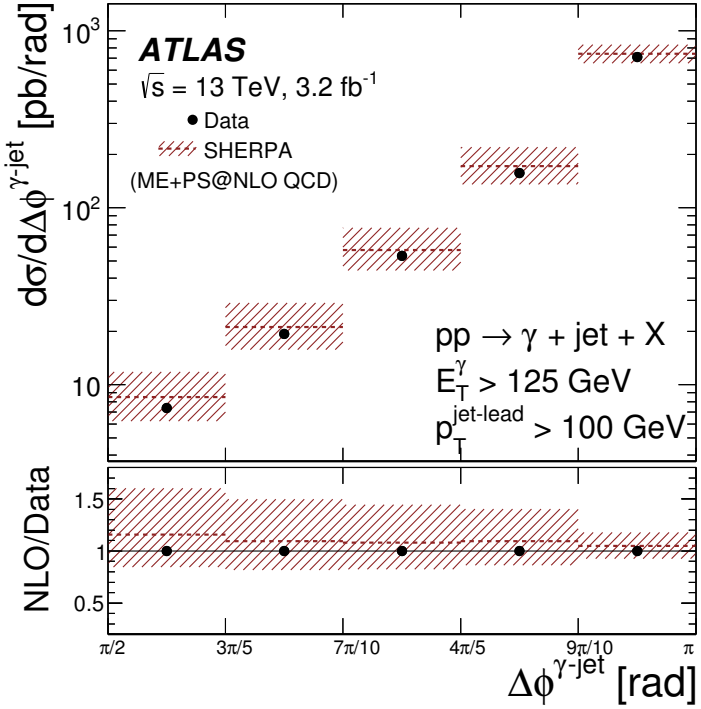

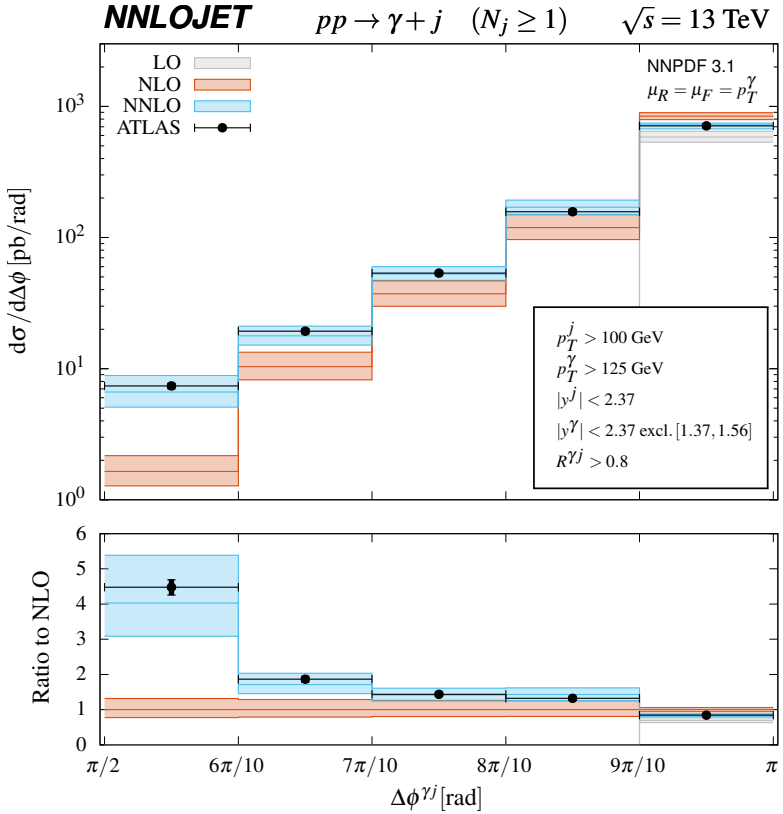

- **Overview of the latest results published by ATLAS in prompt-photon production.**
- **Cross-section ratios @ 8 and 13 TeV:**
  $\rightarrow$ Test of the QCD evolution with $\sqrt{s}$ in inclusive-photon production.
  $\rightarrow$ Very stringent test of pQCD.
- **γ+jet @ 13 TeV:**
  $\rightarrow$ Validity of the description of the dynamics of isolated photon plus jet production up to $\mathcal{O}(\alpha_{\mathrm{EM}}\alpha_{\mathrm{s}}^3)$.
- **New results to come with $\sqrt{s} = 13$ TeV.**

Thank you!

BACK UP

Photon reconstruction and identification in ATLAS

- Photon candidates are reconstructed from clusters of energy in the EM calorimeter (Lead-liquid Argon).

  ↪ Presampler: To correct for losses upstream of the calorimeter.
  ↪ First layer: High granularity in η which allows signal photons identification.
  ↪ Second layer: Collects most of the deposited energy.
  ↪ Third layer: Used to correct for leakage.

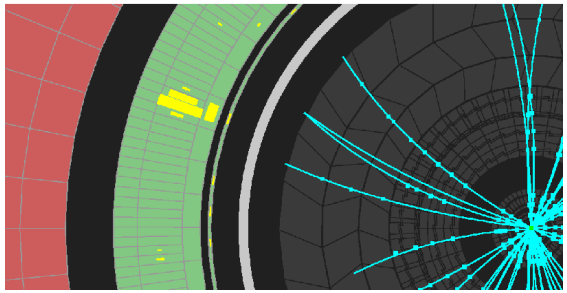

- **"Unconverted"** (cluster of EM cells without matching track) and **"converted"** (clusters of cells with matching track(s) consistent with conversion vertex) photon candidates considered.

- Photon identification from shape variables of the lateral and longitudinal energy profiles of the showers in the calorimeters.

  ↪ **"loose"**: leakage in the hadronic calorimeter, energy ratios and shower width in the 2nd layer.
  ↪ **"tight"**: using also information from the first layer.

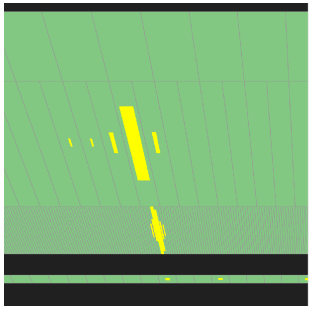

signal photon

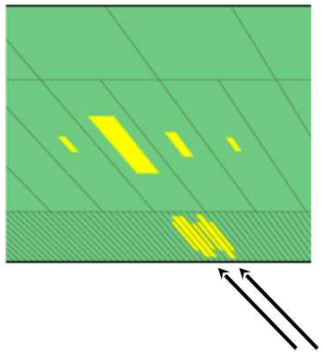

$\pi^0 \to \gamma\gamma$

Jets and flavour-tagging in ATLAS

- Built using the anti-k_t algorithm with radius R=0.4 using topoclusters as input.

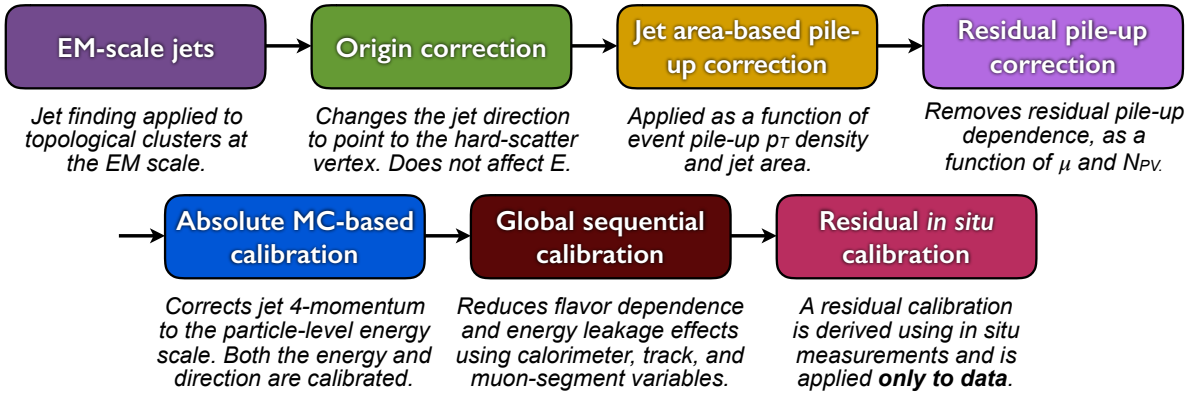

↪ Backgrounds from beam-halo or beam-gas events, cosmic-ray muons or calorimeter noise removed.

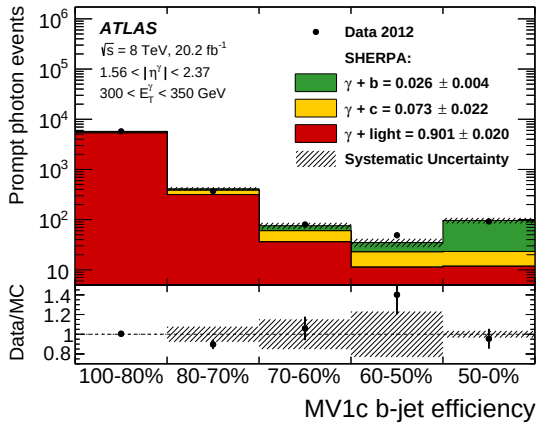

- Flavour-tagging algorithms based on the presence of a secondary vertex or tracks with large impact parameters combined with neural networks to build a discriminant.
- Separate calibration for b-, c- and light jets using $t\bar{t}$, $D^{*\pm}$ or inverting the tagging criteria, respectively.
- Background subtraction in each bin of the measurement and each bin of the discriminant variable.
- Template fits to the discriminant variable to extract the fractions of γ+c and γ+b.

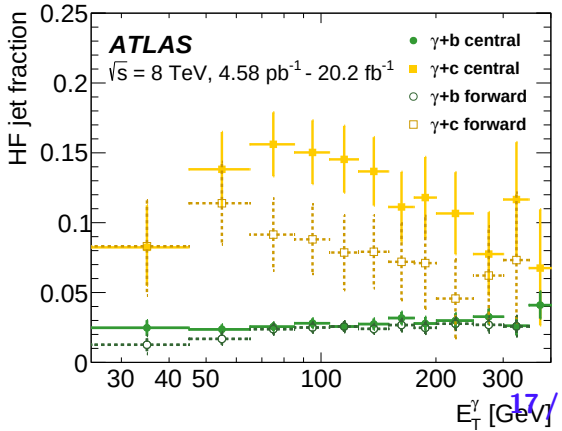

$pp \to \gamma +$ HF at $\sqrt{s} = 8$ TeV

Phys. Lett. B 776 (2018) 295

- First measurement of differential cross section as a function of E_{T}^{γ} in $|\eta^{\gamma}| < 1.37$ and $1.56 < |\eta^{\gamma}| < 2.37$ with $\mathcal{L} = 4.6$ pb^{-1} up to 20.2 fb^{-1}.

$E_{\mathrm{T}}^{\gamma} >$25 GeV, $|\eta^{\gamma}| < 2.37 \notin 1.37 < |\eta^{\gamma}| < 1.56$
$E_{\mathrm{T}}^{\mathrm{iso}} <4.2{\cdot}10^{-3} E_{\mathrm{T}}^{\gamma} + 4.8$ GeV, $\Delta R^{\gamma-\mathrm{j}} > 1.0$
c-/b-tagged jets with $p_{\mathrm{T}}^{\mathrm{jet}} > 20$ GeV, $|y^{\mathrm{jet}}| < 2.5$

- Signal photon purity larger than 60%. Increase with E_{T}^{γ}.
- Background subtraction in each bin of the measurement and each bin of the MV1c discriminant efficiency bin. c and b fractions obtained from template fits to the MV1c tagger distribution.

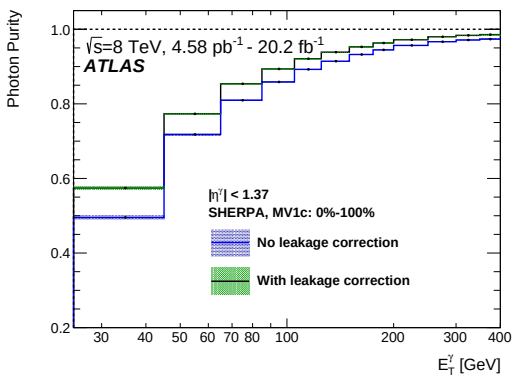

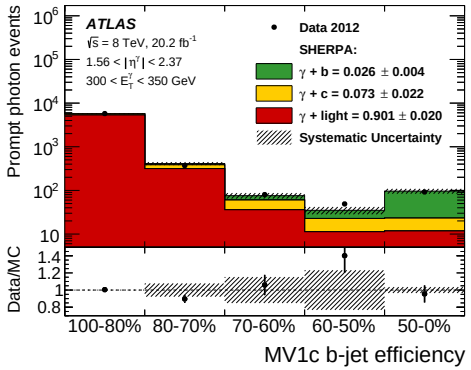

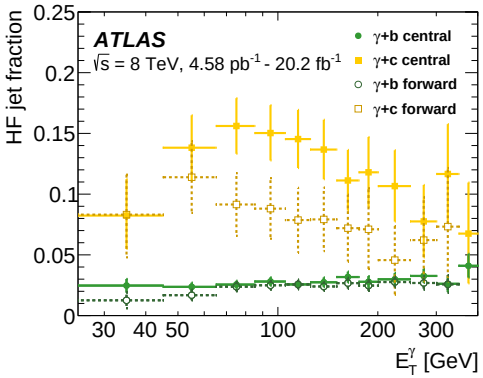

- Dominant systematic uncertainty: flavour tagging efficiency (larger in $\gamma + c$).

Total uncertainty (%)			
$\gamma + b$		$\gamma + c$	
central	forward	central	forward
13–27	14–54	15–62	26–66

$pp \to \gamma +$ HF at $\sqrt{s} = 8$ TeV

Phys. Lett. B 776 (2018) 295

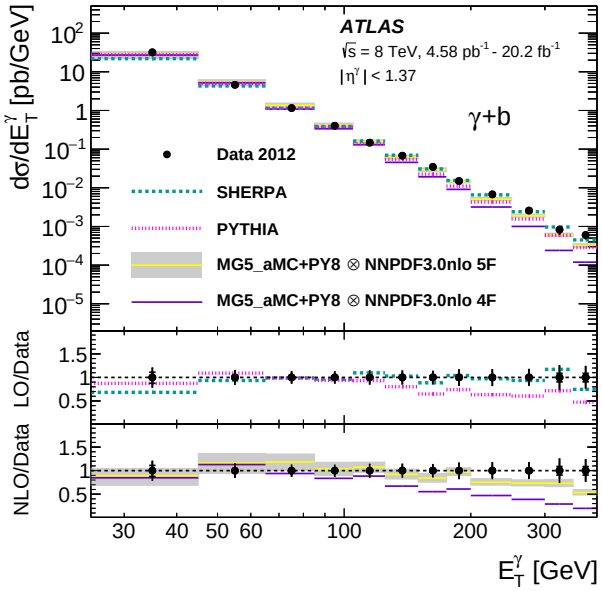

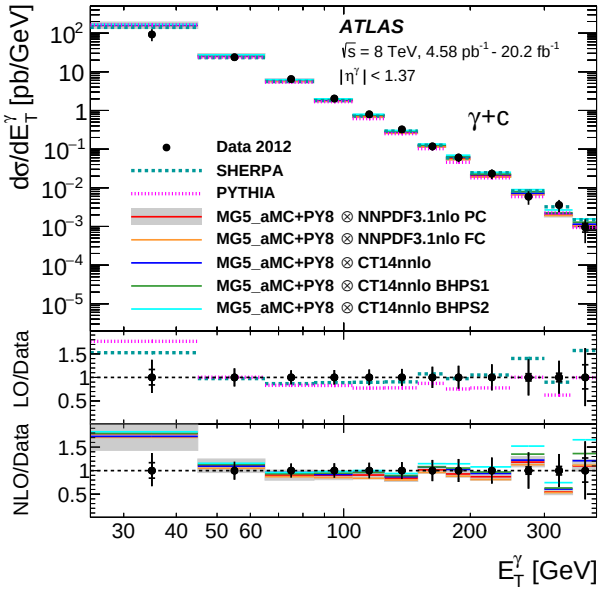

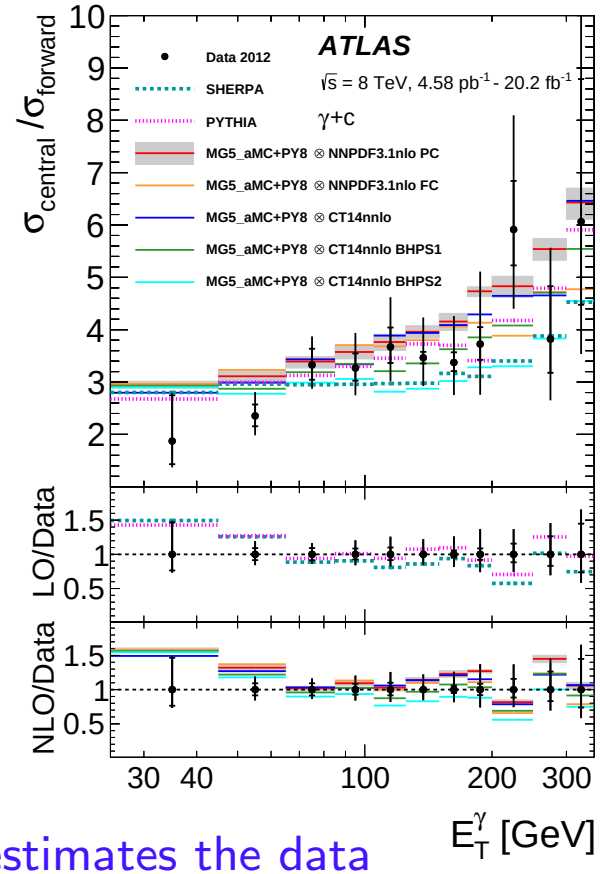

- $\gamma + b$: Madgraph5_aMC@NLO+PYTHIA8 in 4FS underestimates the data above 125 GeV $\to$ better suited for energies close to the b-quark mass.
- Both FS underestimate the data for $E_T^\gamma > 200$ GeV. $\to$ Significant gluon-splitting contribution; only at LO in the 5F scheme.
- Higher-order calculations needed to improve the description of the data.
- $\gamma + c$: Comparisons to PDF sets with different intrinsic charm contribution
- Precision of the measurement comparable to the size of the deviations observed between diffe rent predictions. $\to$ Better precision in the data is needed to discriminate between models.

$pp \to \gamma + \gamma + \gamma$ at $\sqrt{s} = 8$ TeV

PLB 781 (2018) 55

- First measurement of the differential cross sections (SM rare process) as functions of $E_T^{\gamma 1,2,3}$, $\Delta\phi^{\gamma 1,1,2-\gamma 2,3,3}$, $|\Delta\eta^{\gamma 1,1,2-\gamma 2,3,3}|$, $m_{\gamma 1,1,2-\gamma 2,3,3}$ and $m_{\gamma 1\gamma 2\gamma 3}$ with $\mathcal{L} = 20.2$ fb^{-1}

$E_T^{\gamma 1(2,3)} > 27(22,15)$ GeV, $|\eta^\gamma| < 2.37 \notin$
$1.37 < |\eta^\gamma| < 1.56$; $m^{\gamma\gamma\gamma} > 50$ GeV
$E_T^{iso} < 10$ GeV, $\Delta R^{\gamma,\gamma} > 0.45$

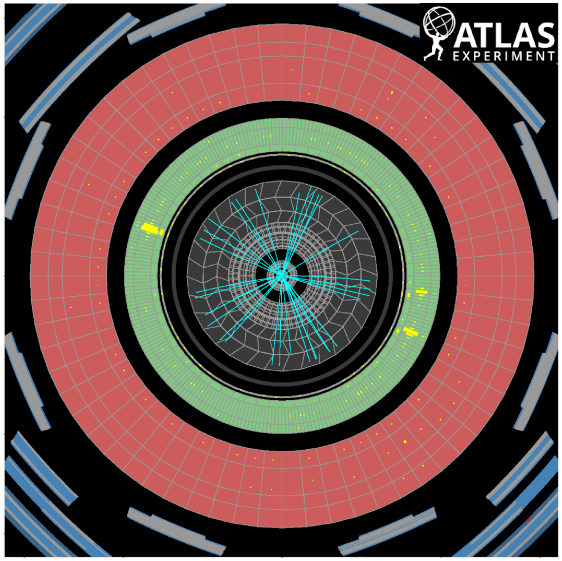

- Dominant systematic uncertainties are related with the background subtraction method and pho ton identification. Statistically limited.

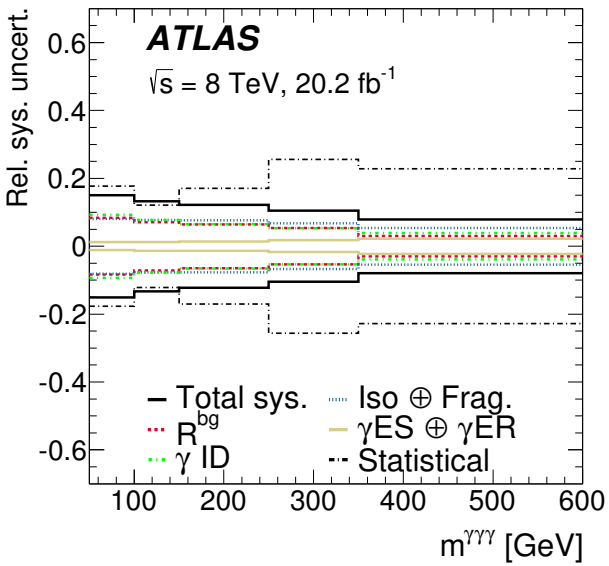

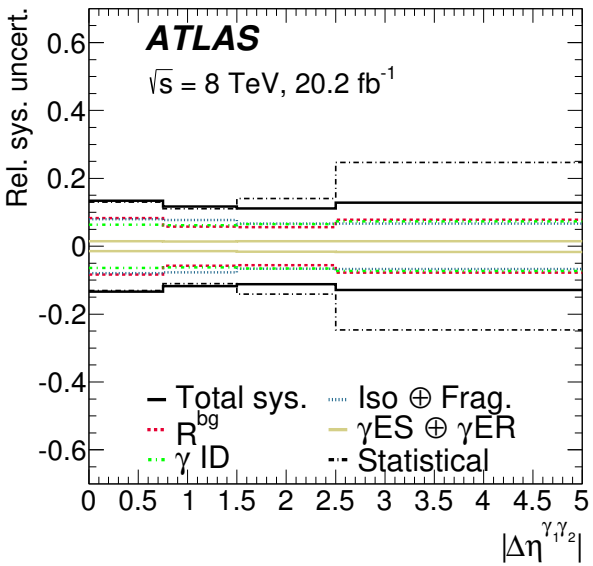

Fiducial cross section

Phys. Lett. B 781 (2018) 55

- Predictions of MCFM
  ↪ NLO pQCD predictions for the direct contribution. Fragmentation contribution at LO.
  ↪ $\mu_R = \mu_F = \mu_f = m^{\gamma\gamma\gamma}$; CT10 PDF; BFGII FF; $\alpha_s(m_Z) = 0.118$; $\alpha_{EM} = 1/137$
  ↪ Corrected for hadronisation and UE effects.

- Predictions of MadGraph5_aMC@NLO
  ↪ NLO pQCD contributions for direct process (Frixione's isolation).
  ↪ Interfaced with PYTHIA8 PS to include ISR and FSR.
  ↪ $\mu_R = \mu_F =$ transverse mass of final-state photons and jets; CT10 PDF; $\alpha_s(m_Z) = 0.118$; $\alpha_{EM} = 1/137$.

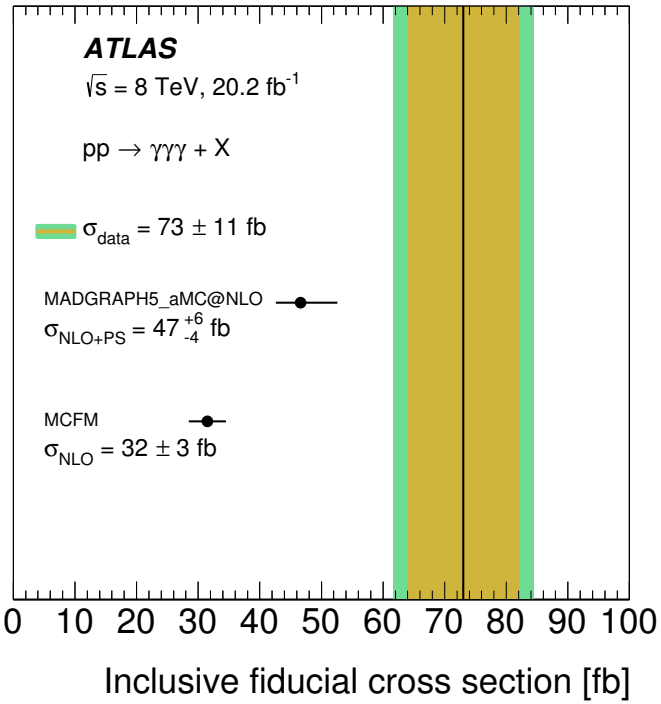

Golden band: systematic uncert.
Green band: syst. + stat. uncert.

- ◇ Theoretical uncertainties include: missing higher orders (dominant), α_s and PDF induced uncertainties and the uncertainty on the non-perturbative corrections for MCFM.
- ◇ Similar discrepancies found for $\gamma\gamma$, $W\gamma\gamma$ and $Z\gamma\gamma$ at NLO
  ↪ Significant improvement by the NNLO for $\gamma\gamma$ (not available for $\gamma\gamma\gamma$).

$pp \to \gamma + \gamma + \gamma$ at $\sqrt{s} = 8$ TeV

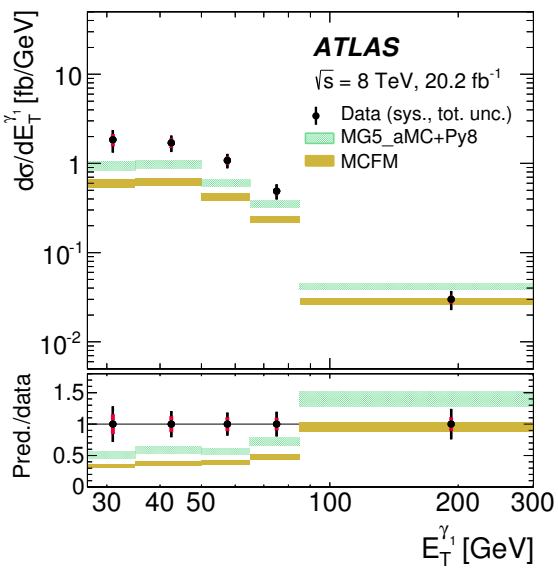

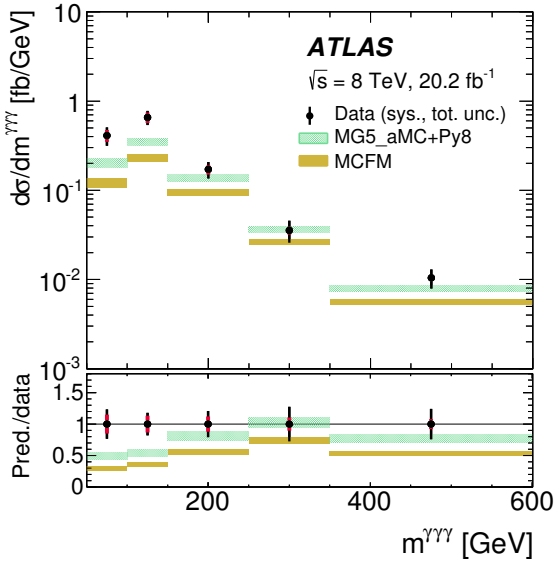

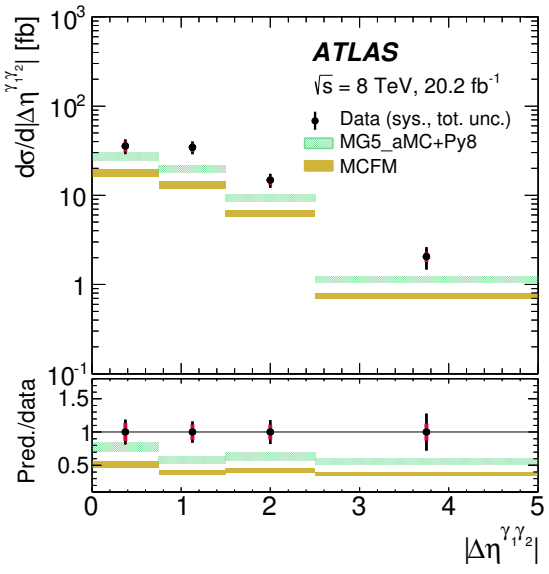

- The NLO calculations fail to describe the shape and normalisation of the distributions in the low E_{T}^{γ} and $m^{\gamma\gamma\gamma}$ regions. Adequate description of the shape of angular variables
  $\hookrightarrow$ Differences up to 60% between data and predictions. Normalisation of MadGraph closer to data and superi or than MCFM describing the shape of $\Delta\phi^{\gamma_1\gamma_2}$
- Need for improved modelling of this process (higher-order corrections).
- Importance of the addition of the parton shower to improve the description of the angular variables.

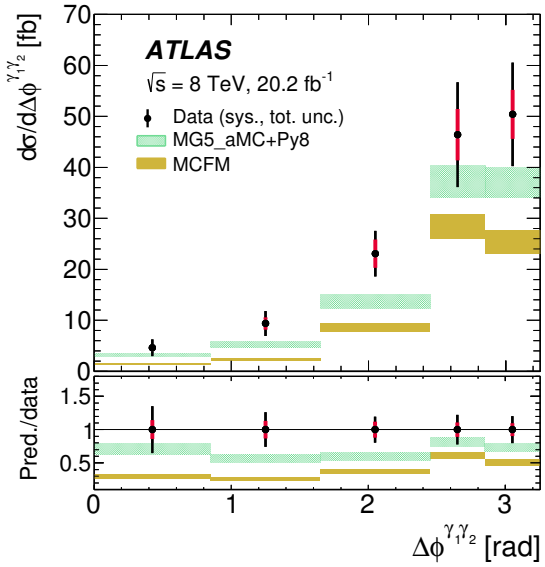

PLB 781 (2018) 55

Direct photon production and PDF fits reloaded

- Direct photon production at NNLO QCD +LL EW; NNPDF3.1NNLO PDF; Frixi one's isolation parameters: $\epsilon = 0.1$, $n = 2$, $R_0 = 0.4$; $\mu_R = \mu_F = E_{\mathrm{T}}^{\gamma}$; $\alpha_{\mathrm{EM}}(m_Z) = 1/127.9$.

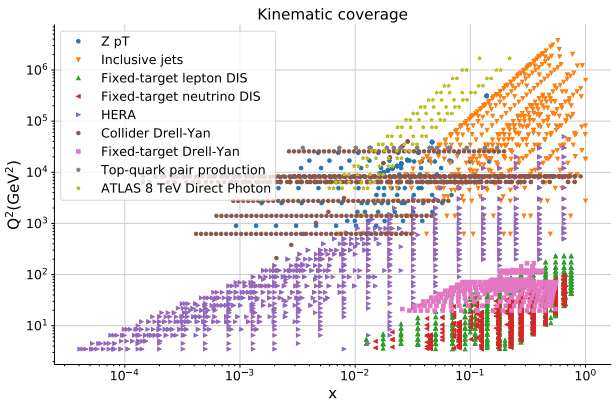

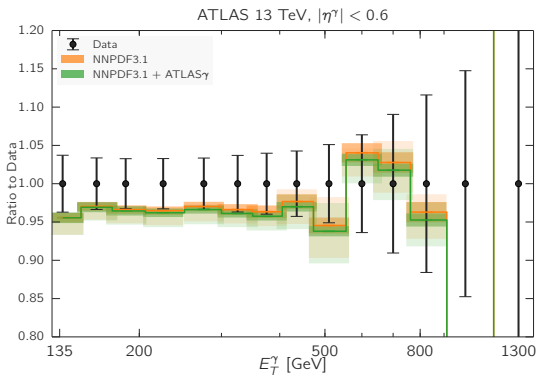

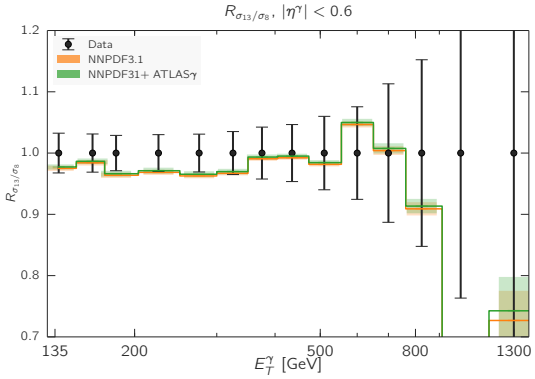

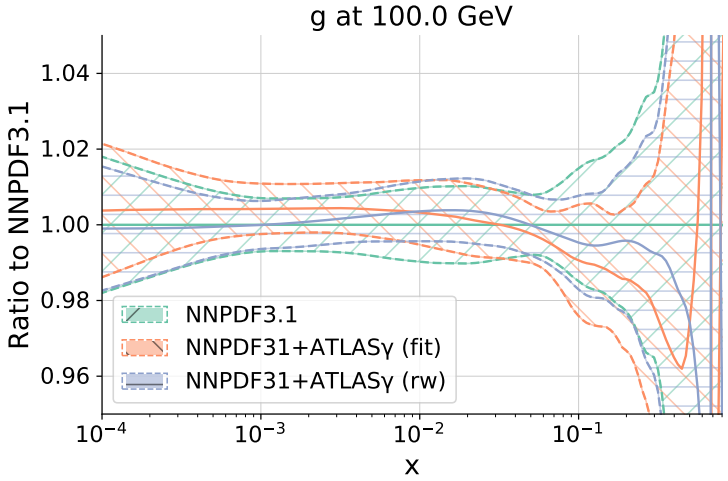

"LHC direct photon production data leads to both a moderate reduction of the gluon uncertainties at medium–x and a preference for a somewhat softer central value at large–x. These effects are more marked when the direct photon data is added on top of fits based on reduced datasets, in particular the NNPDF3.1 no-LHC fit. [...] collider direct photon production should be rightfully restored to its well-deserved position as a full member of the global PDF analysis toolbox."

J. M. Campbell, J. Rojo, E. Slade, C. Williams; arXiv: 1802.03021